

## Ecologically valid combinations of first- and second-order surface markings facilitate texture discrimination

Aaron P. Johnson<sup>a,\*</sup>, Nicolaas Prins<sup>b</sup>, Frederick A.A. Kingdom<sup>c</sup>, Curtis L. Baker Jr.<sup>c</sup>

<sup>a</sup> Department of Psychology, Concordia University, 7141 Sherbrooke Street West, Room SP-245.05 Montréal, Que., Canada H4B 1R6

<sup>b</sup> Department of Psychology, Peabody Building, University of Mississippi University, MS 38677, USA

<sup>c</sup> McGill Vision Research Unit, Department of Ophthalmology, 687 Pine Avenue West Room H4-14, Montréal, Que., Canada H3A 1A1

Received 13 March 2007; received in revised form 7 May 2007

### Abstract

Natural scenes contain localized variations in both first-order (luminance) and second-order (contrast and texture) information. There is much evidence that first- and second-order stimuli are detected by distinct mechanisms in the mammalian visual system. However, in natural scenes the two kinds of information tend to be spatially correlated. Do correlated and uncorrelated combinations of first- and second-order stimuli differentially affect perception? To address this question we employed orientation-modulated textures in which observers were required to discriminate the spatial frequency of the texture modulation. The textures consisted of micropatterns defined as either local variations in luminance (first-order) or luminance contrast (second-order). Performance was robust with textures composed of only first-order micropatterns, but impossible with only second-order micropatterns. However, when the second-order micropatterns were combined with the first-order micropatterns, they enhanced performance when the two were spatially correlated, but impaired performance when the two were spatially uncorrelated. We conclude that local second-order information may enhance texture modulation discrimination provided it is combined with first-order information in an ecologically valid manner.

© 2007 Elsevier Ltd. All rights reserved.

*Keywords:* Texture; Natural images; Image statistics; Second-order; Ecological vision

### 1. Introduction

Natural scenes contain a rich variety of spatial and/or temporal changes in image attributes such as luminance and color, termed first-order information, and in textural attributes such as contrast, spatial frequency and orientation, termed second-order information. A large body of previous research has documented the human visual system's sensitivity to first- and second-order stimuli (Cavanagh & Mather, 1989; Chubb & Sperling, 1998; Landy & Graham, 2004). While first- and second-order image properties are thought to be extracted by different signal processing mechanisms (see below), their relative roles and

interrelationships in visual perception remain poorly understood.

Evidence for distinct processing of first- and second-order visual stimuli comes from neurophysiology, brain lesion studies, neuroimaging and psychophysics (for review see Baker, 1999). Single neurons in cat area 18 respond to both luminance and contrast modulation, often with different spatial and temporal frequency tuning characteristics (Baker & Mareschal, 2001; Mareschal & Baker, 1998; Zhou & Baker, 1996). Neurons in early visual cortical areas also respond to illusory contours defined by abutting gratings (Song & Baker, 2005; von der Heydt & Peterhans, 1989). Lesions in different extrastriate cortical areas result in different degrees of impairment in first- and second-order motion sensitivity (Plant & Nakayama, 1993), in some cases revealing a double-dissociation in sensitivity loss to the two kinds of stimulus (Vaina, Makris, Kennedy, &

\* Corresponding author. Fax: +1 514 848 4545.

E-mail address: [aaron.johnson@concordia.ca](mailto:aaron.johnson@concordia.ca) (A.P. Johnson).

Cowey, 1998). Separate cortical pathways for first- and second-order motion processing are also suggested by functional magnetic resonance imaging (fMRI) studies that reveal distinct extrastriate areas that respond relatively more to first- or to second-order motion (Dumoulin, Baker, Hess, & Evans, 2003; Larsson, Landy, & Heeger, 2006; Smith, Greenlee, Singh, Kraemer, & Hennig, 1998). While all the latter studies found that most early visual areas respond to both forms of motion, Larsson et al. (2006) demonstrated adaptation to each type of motion, but no cross-adaptation in any of these areas. Numerous human psychophysics studies support the idea of separate processing of first- and second-order stimuli. For example, the two kinds of stimuli cannot be integrated to drive motion perception (Ledgeway & Smith, 1994), and do not show cross-adaptation (Larsson et al., 2006; Nishida, Ledgeway, & Edwards, 1997) or cross-facilitation (Schofield & Georgeson, 1999).

While first- and second-order information appears to be detected initially by separate mechanisms, their subsequent processing may be functionally and anatomically linked. For example, human fMRI studies have shown that early visual cortical areas respond similarly to both kinds of stimuli (Dumoulin et al., 2003; Nishida, Sasaki, Murakami, Watanabe, & Tootell, 2003; Smith et al., 1998). Optical imaging studies have shown that orientation columns in V2 are organized into spiral pinwheels which are congruent for the two kinds of stimuli (Ramsden, Hung, & Roe, 2001; Sheth, Sharma, Rao, & Sur, 1996; Zhan & Baker, 2006). Single neurons in early visual cortical areas often respond to borders of either stimulus type, with similar selectivity for orientation, direction of motion and spatial frequency (e.g., Mareschal & Baker, 1998; von der Heydt & Peterhans, 1989).

Although the above studies indicate that the mammalian visual system has specialized mechanisms for processing artificial second-order stimuli, little is known about how second-order information is used by the visual system in more natural situations. Recent studies have demonstrated a wide-spread presence of second-order information in natural images (Johnson & Baker, 2004; Schofield, 2000). Yet in the natural world second-order information is usually correlated with first-order information, with an average correlation of 0.6–0.7 over an ensemble of filtered images (Johnson & Baker, 2004). This correlation likely arises because naturally occurring edges (e.g., occlusion boundaries) are often defined by spatially coincident changes in luminance and texture. A similar correlation also occurs between chromatic first-order and achromatic second-order information, e.g., between coarse-scale color transitions and coarse-scale changes in fine-scale texture (Johnson, Kingdom, & Baker, 2005).

Despite the presence of second-order information within natural scenes and its correlation with first-order information, only a few studies have examined how first- and second-order cues interact when spatiotemporally combined. Smith and Scott-Samuel (2001) showed that for both

spatial-frequency discrimination utilizing static gratings and speed discrimination utilizing drifting gratings, performance was better when the first- and second-order gratings were superimposed (provided they were both presented at low amplitude) compared to when presented alone. Other experiments have shown that while pure second-order motion fails to elicit an optokinetic response (Harris & Smith, 1992, 2000; Lelkens & Koenderink, 1984), when combined with first-order motion oculomotor responses are enhanced (Harris & Smith, 2000). First- and second-order characteristics have also been shown to interact in determining perceived position (Whitaker, McGraw, Keeble, & Skillen, 2004) or orientation (Dakin, Williams, & Hess, 1999; Morgan & Baldassi, 2000). More recently, Schofield, Hesse, Rock, and Georgeson (2006) showed that when a first-order luminance grating was added in-phase with a second-order contrast-modulated texture, the appearance of shape-from-shading was enhanced. On the other hand, when the gratings were combined in anti-phase, the stimulus appeared more-or-less flat.

In this communication, we report experiments investigating how the degree of spatial correlation between first- and second-order information affects performance on a texture discrimination task. We show that task performance either remains the same, or in some cases improves, when second-order information is combined in correlation with first-order information, even though the second-order information by itself fails to elicit above-chance performance. Conversely, when the second-order information is combined with no spatial correlation to the first-order information, task performance is worsened.

## 2. Methods

### 2.1. Subjects

SA was one of the authors (A.J.), while SB and SC were experienced undergraduate volunteers who were naïve as to the purpose of the experiment. All subjects had normal or corrected-to-normal vision. The age of the participants ranged between 18 and 28 years. Informed consent, as approved by the McGill Research Ethics Board, was obtained.

### 2.2. Apparatus

Stimuli were generated using Mathworks' Matlab 6.5 in combination with the Psychophysics Toolbox (Brainard, 1997; Pelli, 1997), running within Microsoft Windows XP (Pentium 4, 2.6 GHz, 1 GB). The stimuli were displayed on a CRT monitor (Sony GDM-F500R, 40.5 × 30 cm, 800 × 600 pixel, 100 Hz, mean luminance 34 cd m<sup>-2</sup>) in all cases except Experiment 4 in which subject SC used a MAG Innovation AH-778 CRT (32 × 24 cm, 800 × 600 pixel, 85 Hz, mean luminance 36 cd m<sup>-2</sup>). The relationship between voltage and screen luminance was measured with a photometer (S370, UDT Instruments) and used to create a video lookup table that linearized the luminance values.

### 2.3. Stimuli

Stimuli were square images (600 pixels or 17.4° at a 100 cm viewing distance on the Sony CRT or 17.2° at 80 cm viewing distance on the MAG CRT), containing a texture composed of quasi-randomly positioned micropatterns added to a background luminance,  $L_0$ . Three types of

micropatterns were employed, one of them luminance-modulated (first-order) and the other two contrast-modulated (second-order). Example micropatterns are illustrated in Figs. 1 and 2. The first-order micropatterns were oriented two-dimensional Gaussians:

$$\text{Gauss}(x, y) = C_F \exp(-1((x'^2/2\sigma_x) + (y'^2/2\sigma_y))) \quad (1)$$

$$x' = x \cos \theta_e + y \sin \theta_e \quad y' = -x \sin \theta_e + y \cos \theta_e$$

where  $C_F$  is a contrast-multiplier,  $\sigma_x$  is the width of the Gaussian envelope, and  $\sigma_y$  is the length of the Gaussian envelope ( $\sigma_y = \sigma_x/2$ ), and  $\theta_e$  the Gaussian envelope orientation. To ensure that the stimulus texture was globally dc-balanced, half of the micropatterns were ‘bright/white’ ( $C_F > 0$ ), while the other half were ‘dark/black’ ( $C_F < 0$ ). The envelope orientation of the Gaussian was modulated according to a sine-wave profile.

Two types of second-order micropatterns were employed. In Experiments 1 and 3, these were second-order Gabor micropatterns:

$$\text{Gabor}(x, y) = \exp((-x'^2/2\sigma_x) + (-y'^2/2\sigma_y)) \cos(2\pi(x''/\lambda) + \varphi) \quad (2)$$

$$x' = x \cos \theta_e + y \sin \theta_e \quad y' = -x \sin \theta_e + y \cos \theta_e$$

$$x'' = x \cos \theta_c + y \sin \theta_c$$

where  $\lambda$  is spatial wavelength (reciprocal spatial frequency, in pixels),  $\varphi$  the phase offset of the sinusoidal carrier ( $\varphi = \pi/2$  or  $3\pi/2$ , with equal probability),  $\sigma_x$  and  $\sigma_y$  (see above) the dimensions of the Gaussian envelope,

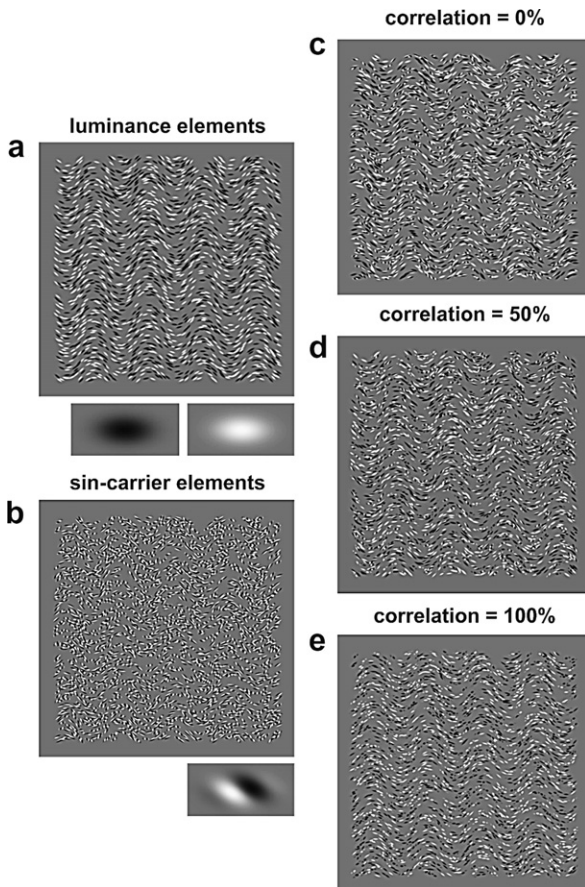


Fig. 1. Examples of texture stimuli with an orientation modulation of 4 cycles/image. (a) Homogeneous first-order stimuli created with oriented ‘skinny’ Gaussian micropatterns (example element orientation is 90°). (b) Homogeneous second-order stimuli composed from Gabor micropatterns with random-oriented sinusoidal luminance carriers (in the example element, carrier orientation is 45° while envelope orientation is 90°). (c–e) Stimuli created with mixtures of first- and second-order Gaussian/Gabor micropatterns, with spatial correlations of 0%, 50% and 100%.

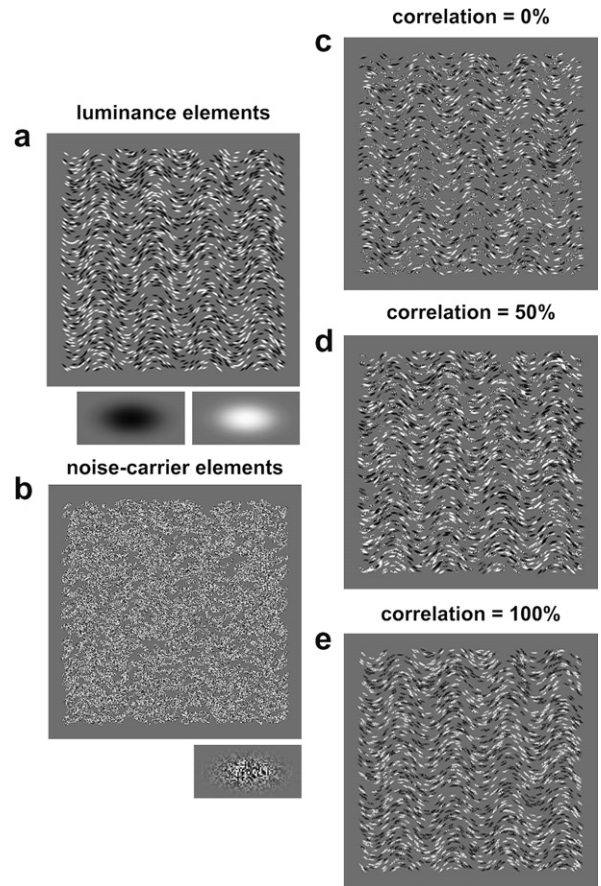


Fig. 2. Same as Fig. 1, but second-order elements consist of orientated Gaussian envelopes which modulate contrast of noise carriers (example element orientation is 90°).

$\theta_c$  envelope orientation and  $\theta_e$  carrier orientation. In these textures (Fig. 1), the micropattern’s envelope orientation was modulated across the texture according to a sine-wave profile, while its (sinusoidal) carrier orientation was set randomly for each micropattern. In Experiments 2, 4 and 5, the second-order micropatterns consisted of random binary noise with a Gaussian contrast modulation envelope (Eq. (1)). Again, it was the orientation of the envelope that was modulated across the texture according to a sine-wave profile (Fig. 2).

In some of the stimuli, the first- and second-order micropatterns were additively superimposed on a background gray luminance,  $L_0$ :

$$\text{image}(x, y) = L_0(1 + C_F \sum (\text{Gauss}_i(x, y)) + C_S \sum (\text{Gabor}_i(x, y))) \quad (3)$$

where  $C_F$  and  $C_S$  are contrast parameters for the Gaussian and Gabor micropatterns, and  $i$  the index number of the micropattern. Because the micropatterns were dc-balanced over the entire image, their Michelson contrasts were  $C_F$  and  $C_S$ , respectively. When the first- and second-order micropatterns were perfectly superimposed, the spatial locations and orientations ( $\theta_e$  in Eqs. (1) and (2)) of their envelopes were identical. In the 100% spatial correlation condition, all first- and second-order micropatterns were superimposed in this way. Reducing the proportion of superimposed micropatterns produced textures with a spatial correlation less than 100%, and with no micropatterns superimposed, the spatial correlation was 0%.

To ensure an approximately uniform texture density across each stimulus and to eliminate overlap, the micropatterns’ positions were constrained to center-to-center separations of at least the width of the envelope ( $\sigma_y$ ). Under this constraint there were 8000 available positions, to which the micropatterns were randomly allocated (only one per

position) for each stimulus presentation. In Experiments 1–4 the stimuli contained 2000 micropatterns, while for Experiment 5 the stimuli contained 1000–2000 micropatterns.

To create the orientation-modulated (OM) textures (e.g., Figs. 1 and 2), the envelope orientations of the micropatterns ( $\theta_c$ ) were modulated according to a sinusoidal function of horizontal position ( $x$ ):

$$\theta_c(x) = A \sin(2\pi fx + \varphi) \quad (4)$$

where  $A$  is modulation depth,  $f$  spatial frequency of orientation modulation and  $\varphi$  phase of modulation. For the textures composed of second-order Gabor micropatterns, the sinusoidal carrier orientations ( $\theta_c$ ) were randomized across micropatterns. Modulation phase ( $\varphi$ ) was also randomized across trials. Fig. 1(a) shows an OM texture made of first-order micropatterns with a modulation frequency of 4 cycles/image (or 0.23 cycles/degree). Fig. 1(b) shows an OM texture made from second-order micropatterns with the same modulation amplitude; note how the micropattern envelopes follow the sinusoidal texture modulation while the carriers are randomly oriented. Figs. 1 c, d and e show first- and second-order micropatterns with varying degrees of correlation (0%, 50%, 100%). Figs. 2a–e show the same arrangements as in Fig. 1, except using second-order elements composed of contrast-modulated noise.

#### 2.4. Procedure

Observers viewed the screen binocularly and fixated on a centrally located target. Each observer-initiated trial consisted of two OM stimuli, each presented for 500 ms, separated by a 500 ms blank interval at the mean gray luminance ( $L_0$ ). Observers indicated through a button press which of the two displayed patterns contained the higher OM spatial frequency ( $f$ ) in a temporal two-alternative forced-choice procedure. On each trial, one presentation was at the base OM spatial frequency (4 cycles/image), and the other at one of five different values (4.2, 4.4, 4.6, 4.8, 5.0 cycles/image), corresponding to Weber ratios ( $W_r$ ) of 0.05, 0.10, 0.15, 0.20, 0.25, selected in random order. Blocks of 50 trials consisted of 10 randomly selected instances of the five Weber ratios. For each block of trials, a psychometric function of proportion correct versus Weber ratio was fit with a logistic function,  $0.5 + 0.5/(1 + \exp(-(X - a)/b))$ , with  $a$  the Weber ratio threshold at 75% correct and  $1/b$  determining the slope. The functions were fit using Sigmaplot 8.0 (Systat Software Inc.). This procedure was repeated 10 or more times, after which final threshold estimates and standard errors were derived from the individual estimated thresholds.

Feedback via an auditory tone for an incorrect response was provided during initial familiarization trials, where the Weber ratio between the two presentations was fixed at 5.2 cycles/image. Subsequent measurement trials were conducted without feedback as attention and performance had been optimized by the familiarization trials.

### 3. Results

#### 3.1. Experiment 1: OM spatial-frequency discrimination in textures consisting of first-order Gaussians and second-order Gabors

Fig. 3 shows psychometric functions for subjects SA (Fig. 3a), and SB (Fig. 3c). Percent correct OM spatial-frequency discrimination ( $P_{\text{correct}}$ ) is plotted as a function of the Weber OM spatial-frequency ratio. Each plot shows data for OM textures made from either first-order Gaussian micropatterns (solid circles), second-order Gabor micropatterns with random carrier orientations (open circles), first- and second-order micropatterns with zero envelope correlation (solid squares), first- and second-order micropatterns with 50% envelope correlation (open squares),

and first- and second-order micropatterns with 100% envelope correlation i.e., fully superimposed (closed triangles). Both subjects were able to perform the envelope OM spatial-frequency discrimination task at better than chance levels with textures composed of only first-order Gaussian micropatterns (except at the lowest Weber ratio). However, when the stimulus consisted of only second-order micropatterns (Gabor with random carrier orientation), subjects performed no better than chance. When the textures contained both first- and second-order micropatterns that were not correlated (i.e., micropattern envelopes were not superimposed), performance was significantly worse compared to the condition in which the texture contained only first-order micropatterns. However, as the correlation between the first- and second-order micropatterns was increased to 50%, performance increased (left-shift) to the only-first-order-micropattern level. Best performance was achieved for textures comprised of 100% correlated first- and second-order micropatterns (closed triangles, Figs. 2a and c). The increase in performance with the degree of correlation is shown more clearly in Figs. 3b and d, where the threshold Weber ratios ( $W_{75}$ ) for all five conditions are presented. In both subjects, the  $W_{75}$  threshold is smallest for the textures with 100% correlation between first- and second-order patterns, and greatest for the textures with 0% correlation. The  $W_{75}$  threshold for textures created from only first-order micropatterns, and 50% correlation between first- and second-order patterns, fall between these two extremes.

#### 3.2. Experiment 2: OM spatial-frequency discrimination in textures combining first-order Gaussian with second-order contrast-modulated noise micropatterns

Fig. 4 shows psychometric functions obtained when the second-order micropatterns were constructed from contrast-modulated noise, again for subjects SA (Fig. 4a) and SB (Fig. 4c). The results are similar to those of Experiment 1. The subjects were able to perform the task only if first-order micropatterns were present. Again, increasing the degree of correlation between the first- and second-order micropatterns improved performance, at 100% correlation to a level surpassing that found when only first-order micropatterns were present (Figs. 4b and d).

#### 3.3. Experiment 3: OM spatial-frequency discrimination in textures with spatially overlapping but not orientationally co-aligned first- and second-order micropatterns

For the 100% correlation condition in Experiments 1 and 2, the first- and second-order micropattern envelopes were superimposed, i.e., correlated in both spatial position and orientation. Here, we ask whether the improved performance when the first- and second-order micropatterns were superimposed was due to their *orientational co-alignment* or their *spatial overlap*. We repeated the conditions of Experiment 1, except that the orientations of either the

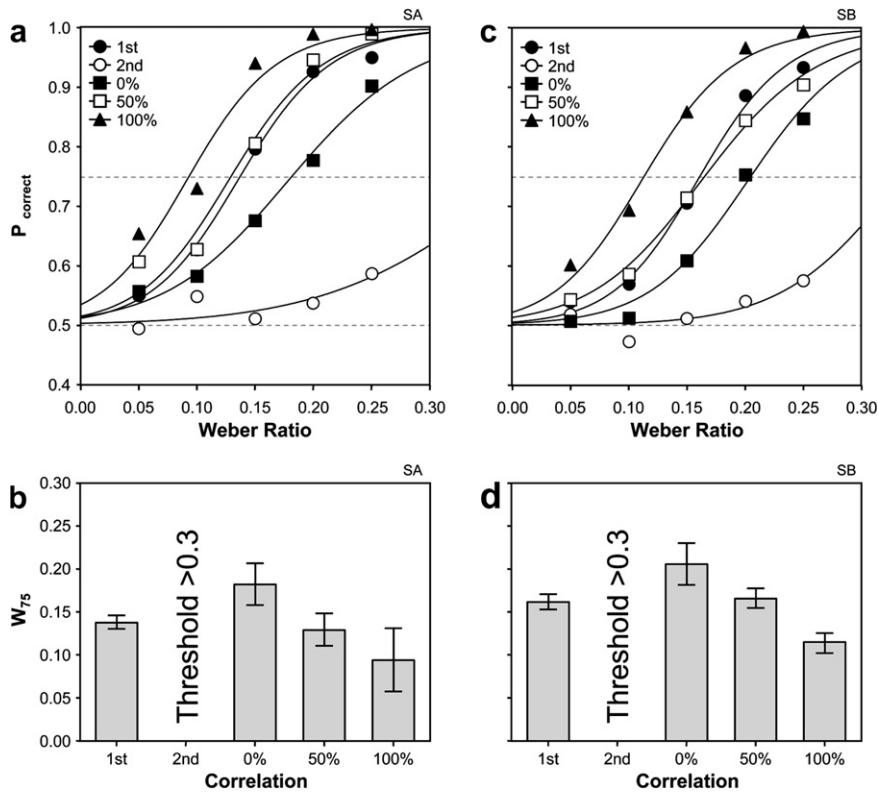


Fig. 3. Spatial-frequency modulation discrimination for OM textures. (a) Psychometric functions of spatial-frequency discrimination expressed as Weber ratios (base frequency, 4 cycles/image), for textures created with first-order Gaussian micropatterns (solid circles), second-order Gabor micropatterns (open circles), 0% correlation between first- and second-order micropatterns (solid square), 50% correlation (open square) and 100% correlation (solid triangle) between first- and second-order elements. Data fitted with logistic psychometric function using a logistic function (see procedure). (b) Weber ratio estimates for 75% response thresholds ( $W_{75}$ ) obtained from the psychometric functions in (a). Error bars indicate standard error. (c,d) As in (a,b) but for a different subject.

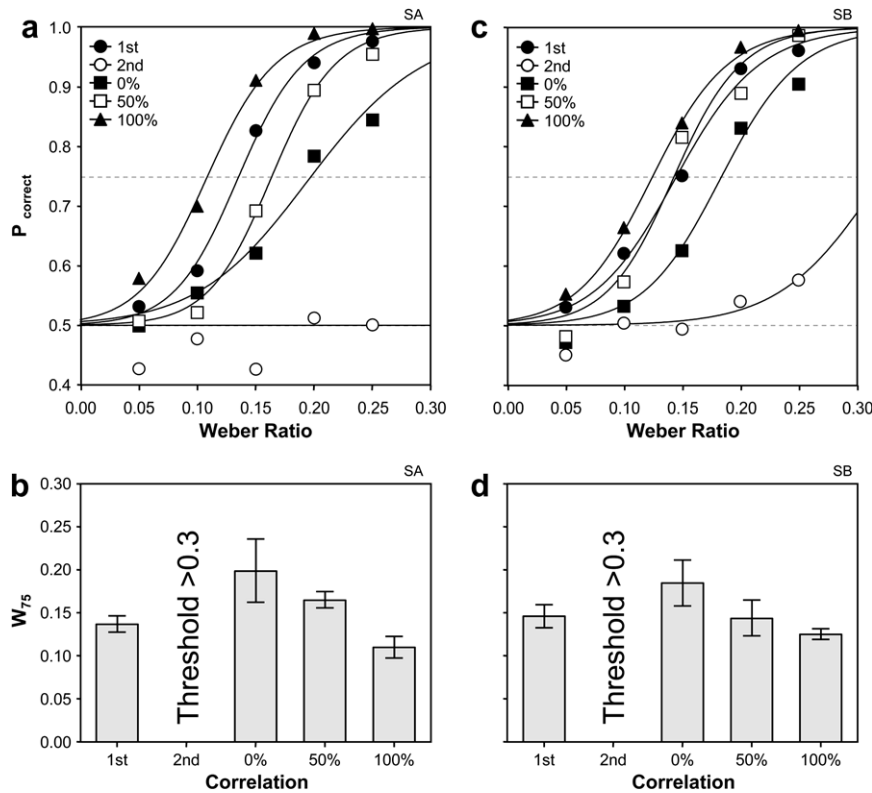


Fig. 4. Same as Fig. 3 except second-order elements consist of orientated Gaussian envelopes which modulate contrast of noise carriers (as in Fig. 2).

first-order (Figs. 5a and c) or second-order micropattern envelopes (Figs. 5b and d) were randomized, thus creating first- and second-order micropatterns that were spatially overlapping (50% or 100%), but not orientationally aligned. When the first-order micropattern orientations were randomized, such that only the second-order micropatterns defined the sine-wave modulation, subjects were unable to perform the task (no better than chance at all five Weber ratios). These results parallel the previous findings for second-order only micropatterns (Fig. 3). When the orientations of the second-order only micropatterns were randomized (Figs. 5b and d), so that only the first-order micropatterns defined the sine-wave modulation, performance was reduced in comparison to that obtained with only first-order micropatterns (Fig. 3). With zero spatial overlap, the results are similar to Experiments 1 and 2, i.e., a performance decrease in comparison to the first-order only micropattern condition. However, unlike Experiments 1 and 2, increasing the spatial overlap from 0% to 100% decreased performance. This shows that the benefit of superimposing second-order onto first-order micropatterns only occurs when they are orientationally aligned. Note however that at 100% spatial overlap, subjects

performed better than chance, albeit only at the two highest Weber ratios (equivalent to 4.8 and 5 orientation modulations per image).

### 3.4. Experiment 4: Effect of correlation in more detail

In the first three experiments, we showed that increasing the correlation between the first- and second-order micropatterns systematically improved performance, provided the increase in correlation took the form of an increase in orientation alignment. Previously, we reported that first- and second-order features in natural images are correlated, up to a correlation of about 0.7 (Johnson et al., 2005). Experiment 2 revealed that the correlation between first- and second-order micropatterns can affect a psychophysical task. To study the effect of correlation more closely, we repeated Experiment 2, but with the addition of textures having 25% and 75% correlation. Fig. 6 shows the resulting psychometric functions for SA (Fig. 6a), and (naïve) subject SC (Fig. 6c). As the correlation increases, performance improves. In one subject (SA), the performance appears to asymptote at 75% correlation. The second subject (SC)

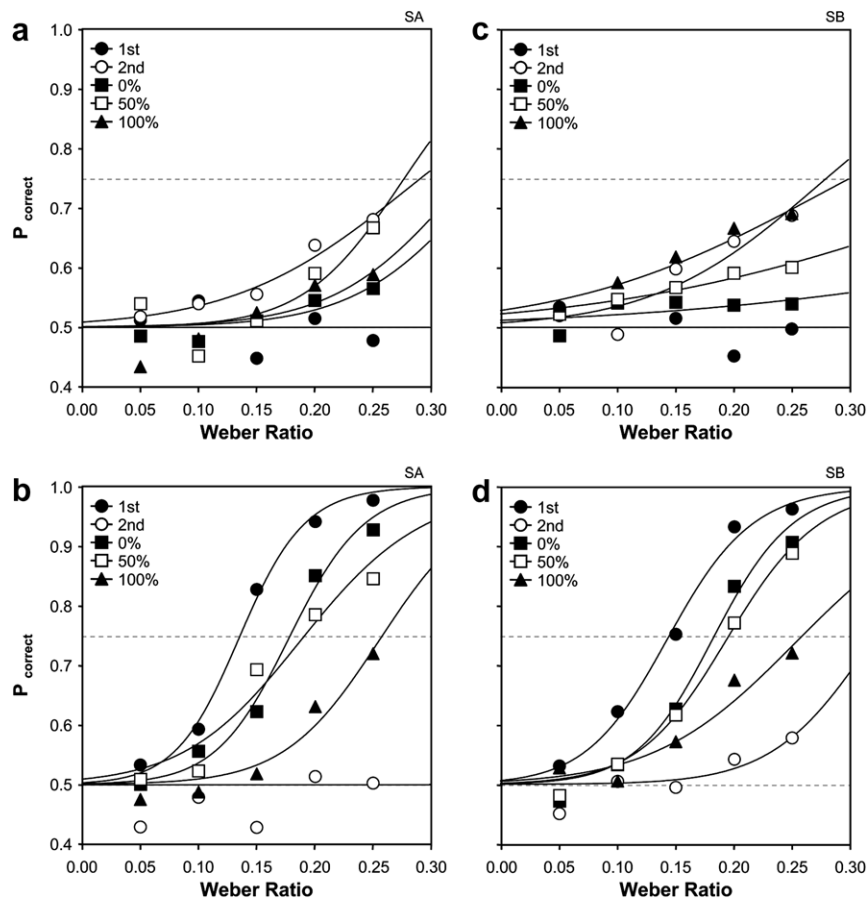


Fig. 5. Spatial-frequency discrimination for textures consisting of first- and second-order micropatterns that are spatially overlapping but not orientationally aligned. The results are shown in the same format as the top graphs in Figs. 3 and 4. (a) The textures are the same as those shown in Fig. 3, except that the first-order micropatterns have random orientations. (b) Textures again as in Fig. 3, except that the second-order micropatterns have random orientations (c, d). As in (a, b) but for a different subject.

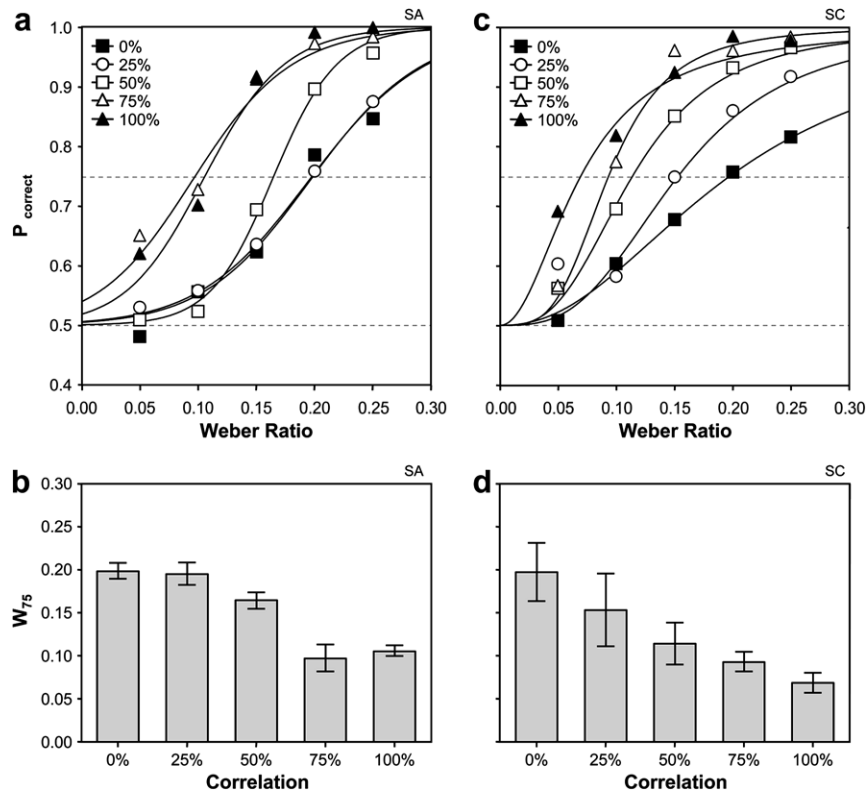


Fig. 6. Effect of correlation between first- and second-order elements on spatial-frequency discrimination. (a) Psychometric functions, shown in same format as previous figures. Correlation between first-order (Gaussian) and second-order (CM noise) elements was varied between 0% and 100% in 25% increments. (b) Weber ratio estimate for 75% response thresholds ( $W_{75}$ ) from psychometric functions in (a). Error bars indicate standard error. (c,d) Same as (a,b) but for a different subject.

shows a similar trend, but does not reveal a clear asymptote in task performance at 75% correlation.

### 3.5. Experiment 5: Effect of contrast and micropattern density

We consider two possible subsidiary reasons why performance might have increased with first- and second-order micropattern correlation. The first is the increase in peak micropattern contrast micropattern superimposition. Our motivation for this control experiment was to investigate whether the performance increase in the correlated conditions was caused by some increase in local signal contrast in correlated micropatterns, in comparison with isolated micropatterns. To test this possibility, we repeated the 100% correlation condition in Experiment 2, at full contrast ( $C_F$  and  $C_S = 0.5$ , closed circles) and at 50% contrast ( $C_F$  and  $C_S = 0.25$ , open circles). Fig. 7a shows the psychometric functions. The result for the 50% contrast condition is similar to the normal contrast condition which was used through the previous experiments. Therefore, the beneficial effects of correlation do not appear to be due to local variations in contrast.

Another possibility is that as the micropattern correlation is increased, there is a corresponding decrease in micropattern coverage, which might result in improved

performance because the signal elements become more salient. We tested this by repeating the 100% correlation condition in Experiment 2 but with two different micropattern densities: 1000 and 2000 micropatterns per image. The two micropattern densities correspond to the 0% (i.e., 2000 micropatterns) and 100% (1000 micropatterns) correlation conditions in Experiment 2. Fig. 7c shows the psychometric functions and Fig. 7d  $W_{75}$  thresholds. The results show that similar psychometric functions were obtained in the 1000 and 2000 micropattern conditions. Therefore the performance increase with correlation does not appear to be related to the change in micropattern coverage.

## 4. Discussion

There are four main findings. First, subjects can discriminate the spatial frequency of OM textures composed of first-order, but not of second-order micropatterns. Second, when OM textures are comprised of first- and second-order micropatterns that are not correlated, performance is worse compared to when the textures are comprised of only first-order micropatterns. This is true whether the second-order micropatterns are defined as random-carrier Gabors or as contrast-modulated noise. Third, increasing the spatial correlation between the first- and second-order micropatterns systematically improves performance. At 50% correlation,

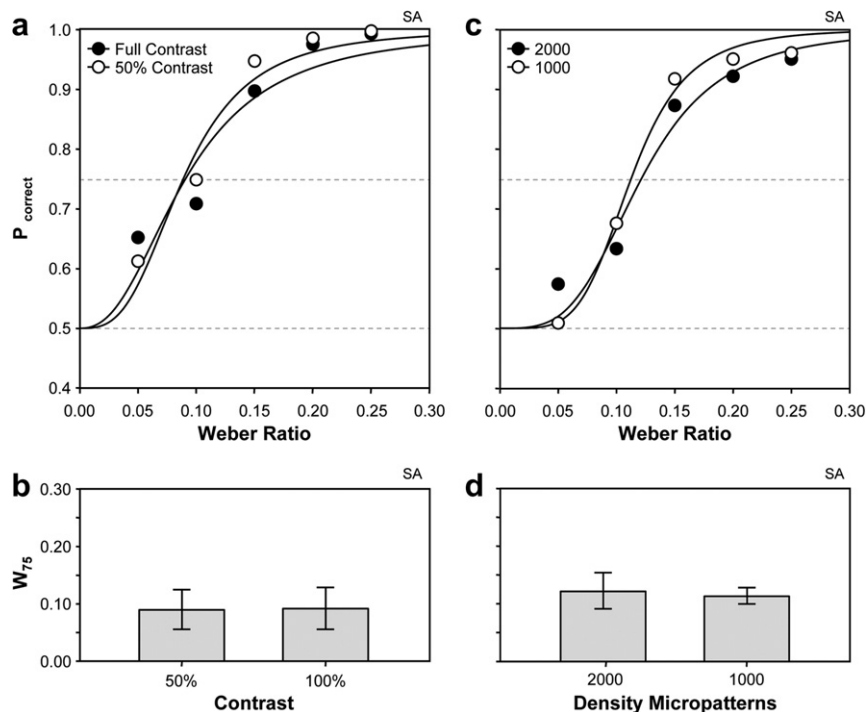


Fig. 7. (a,b) Effect of contrast on spatial-frequency discrimination using textures with 100% correlation between first- and second-order elements. Psychometric functions (a) and 75% response thresholds (b) shown in same format as previous figures for Michelson contrasts at 50% (0.25) and full contrast (0.5). (c,d) Effect of micropattern density on spatial-frequency discrimination using textures with 100% correlation between first- and second-order elements. Psychometric functions (c) and 75% response thresholds (d) shown in same format as previous figures, with either 1000 or 2000 micropatterns.

task performance is equivalent to that for textures comprised of only first-order patterns. At 75% and 100% correlation, performance is higher than with just first-order micropatterns. Fourth, the beneficial effects of spatial correlation are not due to (a) spatial overlap, as opposed to orientational co-alignment, (b) increase in micropattern contrast or (c) decrease in micropattern density.

Can any of these results be attributable to differences in the information content of the stimuli? Consider how an ideal observer would fare in identifying the interval containing the 4 cycles/image stimulus. Recall that the orientations of the signal micropatterns were not stochastically generated; they were determined solely by their positions along the  $x$ -axis of the OM waveform, given the waveform's mean, amplitude, spatial frequency and phase. In Experiment 3, where the orientations of one of the types of micropattern were randomized, these would simply be ignored by an ideal observer as they were of a different type from the signal micropatterns. Although the positions of the micropatterns were quasi-random (see Section 2), the ideal observer, because it knows the mean and amplitude of the waveform, would only need to measure (a) the orientations of two signal micropatterns at different points along the  $x$ -axis of the waveform and (b) their horizontal separation, to determine whether or not the stimulus was 4 cycles/image. Note that such a computation would deliver the waveform phase as well as spatial frequency, so the fact that phase was randomized would not introduce any uncer-

tainty for the ideal observer. Except for the effects of photon noise, which would be minimal, there is therefore no uncertainty as regards the signal, and ideal observer performance would be near-perfect in all conditions. Therefore any differences in performance between the different conditions must be due to differences in visual processing, not information content.

Numerous studies have demonstrated that the combination of more than one cue to a percept can lead to improved performance. For example: luminance spatial frequency, contrast and orientation combine to improve the localizability of a texture-defined edge (Landy & Kojima, 2001); texture and disparity combine to improve the perception of slant (Hillis, Watt, Landy, & Banks, 2004); luminance and color combine to promote perceived shape-from-shading (Kingdom, 2003). Other studies have explicitly considered whether first- and second-order cues combine, for example, for motion detection (Smith & Scott-Samuel, 2001). Models of "cue combination" typically involve a weighted sum of signals from mechanisms that separately encode the different cues. Our results differ from conventional cue combination predictions in two ways. First, one of the cues, the information from second-order micropatterns, is unable to support performance on its own. Second, combining the cues can be beneficial, detrimental or neutral, depending on their joint image statistics. This suggests that signals from first- and second-order information are combined non-linearly. Other studies have also shown that second-order information on its



own may fail to produce a perceptual response, e.g., the optokinetic response (Harris & Smith, 1992, 2000; Lelkens & Koenderink, 1984), and other studies have also demonstrated non-linear, i.e., interacting combinations of first- and second-order cues (Dakin et al., 1999; Morgan & Baldassi, 2000; Whitaker et al., 2004).

#### 4.1. Information interacts in human perception performance

Why would the human visual system be sensitive to spatial correlations of two (or more) types of image statistics? In natural images both first- and second-order stimulus components are often spatially correlated, e.g., objects often differ from their backgrounds in both luminance, color, contrast and texture (Johnson & Baker, 2004; Johnson et al., 2005). Martin, Fowlkes, and Malik (2004) have shown that a computer vision algorithm designed to detect object boundaries in natural scenes performs optimally when brightness (luminance), texture and color cues are combined. They showed that by combining these cues, the algorithm's performance approaches that of figure-ground segmented maps produced by human observers. Although the algorithm performance is not as good as the ground truth maps, its performance better corresponds to that of humans compared to traditional image processing algorithms based only on luminance modulations. This suggests that the human visual system combines these cues to help segment objects from one another.

Correlation between cues is also well suited to provide information about the properties (Johnson et al., 2005) and shapes of object surfaces. In natural scenes, luminance changes that are spatially correlated with hue and/or texture changes tend to be associated with occlusion boundaries or with changes in surface reflectance, whereas those that are uncorrelated with hue and/or texture changes tend to originate from non-uniform illumination, such as shadows and shading (Kingdom, 2003; Schofield et al., 2006). Schofield et al. (2006) showed that the form of correlation between luminance and contrast modulation can affect the perceived shape and depth of an object: perceived depth was greatest when the texture's luminance modulation (LM) and the amplitude modulation (AM) were combined in-phase (LM + AM, i.e., correlated), and least when they were combined in anti-phase (LM–AM, i.e., negatively correlated).

We have previously shown that statistical analyses of natural scenes reveal a correlation between luminance/color information and texture/contrast information (Johnson & Baker, 2004; Johnson et al., 2005). It has been proposed that the sensory system has evolved to exploit the statistical invariances observed in natural scenes (review: Simoncelli & Olshausen, 2001). Our findings agree with this idea, and show that perceptual performance in a task consisting of both first- and second-order information is best when the two sources of information are presented in ecologically valid combinations.

#### Acknowledgments

An early report of these findings was presented at the annual meeting of the Visual Sciences Society in May, 2006 (Johnson, Prins, Kingdom, & Baker, 2006). This work was funded by a grant from the Natural Sciences and Engineering Research Council of Canada to CB (OPG-0001978) and to FK (OGP-01217130).

#### References

- Baker, C. L. Jr., (1999). Central neural mechanisms for detecting second-order motion. *Current Opinion in Neurobiology*, 9, 461–466.
- Baker, C. L., Jr., & Mareschal, I. (2001). Processing of second-order stimuli in the visual cortex. In C. Casanova & M. Ptito (Eds.). *Vision: From Neurons to Cognition (Progress in Brain Research)* (Vol. 134, pp. 78–89). Elsevier.
- Brainard, D. H. (1997). The Psychophysics Toolbox. *Spatial Vision*, 10, 433–436.
- Cavanagh, P., & Mather, G. (1989). Motion: The long and short of it. *Spatial Vision*, 4, 103–129.
- Chubb, C., & Sperling, G. (1998). Drift-balanced random stimuli: a general basis for studying non-Fourier motion perception. *Journal of the Optical Society of America A*, 5, 1986–2007.
- Dakin, S. C., Williams, C. B., & Hess, R. F. (1999). The interaction of first- and second-order cues to orientation. *Vision Research*, 39, 2867–2884.
- Dumoulin, S. O., Baker, C. L., Jr., Hess, R. F., & Evans, A. C. (2003). Cortical specialization for first- and second-order motion. *Cerebral Cortex*, 13, 1375–1385.
- Harris, L. R., & Smith, A. T. (1992). Motion defined exclusively by second-order characteristics does not evoke optokinetic nystagmus. *Visual Neuroscience*, 9, 565–570.
- Harris, L. R., & Smith, A. T. (2000). Interactions between first- and second-order motion revealed by optokinetic nystagmus. *Experimental Brain Research*, 130, 67–72.
- Hillis, J. M., Watt, S. J., Landy, M. S., & Banks, M. S. (2004). Slant from texture and disparity cues: Optimal cue combination. *Journal of Vision*, 4, 967–992.
- Johnson, A. P., & Baker, C. L. Jr., (2004). First- and second-order statistics of natural images: A filter-based approach. *Journal of the Optical Society of America A*, 21, 913–925.
- Johnson, A. P., Kingdom, F. A. A., & Baker, C. L. Jr., (2005). Spatiochromatic statistics of natural scenes: First- and second-order information and their correlational structure. *Journal of the Optical Society of America A*, 22, 2050–2059.
- Johnson, A. P., Prins, N., Kingdom, F. A. A., & Baker, C. J. Jr., (2006). Ecological validity determines the impact of second-order information on perceptual performance. *Journal of Vision*, 6, 586.
- Kingdom, F. A. A. (2003). Colour brings relief to human vision. *Nature Neuroscience*, 6, 641–644.
- Landy, M., & Graham, N. (2004). Visual perception of texture. In L. M. Chalupa & J. S. Werner (Eds.). *The Visual Neurosciences* (Vol. 2, pp. 1106–1118). MIT Press.
- Landy, M. S., & Kojima, H. (2001). Ideal cue combination for localizing texture-defined edges. *Journal of the Optical Society of America A*, 18, 2307–2320.
- Larsson, J., Landy, M. S., & Heeger, D. J. (2006). Orientation-selective adaptation to first- and second-order patterns in human visual cortex. *Journal of Neurophysiology*, 95, 862–881.
- Ledgeway, T., & Smith, A. T. (1994). Evidence for separate motion-detecting mechanisms for first- and second-order motion in human vision. *Vision Research*, 34, 2427–2740.
- Lelkens, A. M., & Koenderink, J. J. (1984). Illusory motion in visual displays. *Vision Research*, 24, 1083–1090.
- Martin, D., Fowlkes, C., & Malik, J. (2004). Learning to detect natural image boundaries using local brightness, color and texture cues. *IEEE*

- Transactions on Pattern Analysis and Machine Intelligence*, 26, 530–549.
- Mareschal, I., & Baker, C. L. Jr., (1998). Temporal and spatial response to second-order stimuli in cat A18. *Journal of Neurophysiology*, 80, 2811–2823.
- Morgan, M. J., & Baldassi, S. (2000). Are there separate Fourier and non-Fourier mechanisms for orientation discrimination? *Vision Research*, 40, 1751–1763.
- Nishida, S., Sasaki, Y., Murakami, I., Watanabe, T., & Tootell, R. B. (2003). Neuroimaging of direction-selective mechanisms for second-order motion. *Journal of Neurophysiology*, 90, 3242–3254.
- Nishida, S., Ledgeway, T., & Edwards, M. (1997). Dual multiple-scale processing for motion in the human visual system. *Vision Research*, 37, 2685–2695.
- Pelli, D. G. (1997). The VideoToolbox software for visual psychophysics: Transforming numbers into movies. *Spatial Vision*, 10, 437–442.
- Plant, G. T., & Nakayama, K. (1993). The characteristics of residual motion perception in the hemifield contralateral to lateral occipital lesions in humans. *Brain*, 116, 1337–1353.
- Ramsden, B. M., Hung, C. P., & Roe, A. W. (2001). Real and illusory contour processing in area V1 of the primate: A cortical balancing act. *Cerebral Cortex*, 11, 648–665.
- Schofield, A. J., & Georgeson, M. A. (1999). Sensitivity to modulations of luminance and contrast in visual white noise: Separate mechanisms with similar behaviour. *Vision Research*, 39, 2697–2716.
- Schofield, A. J. (2000). What does second-order vision see in an image? *Perception*, 29, 1071–1086.
- Schofield, A. J., Hesse, G. S., Rock, P. B., & Georgeson, M. A. (2006). Local luminance amplitude modulates the interpretation of shape-from-shading in textured surfaces. *Vision Research*, 46, 3348–3462.
- Sheth, B. R., Sharma, J., Rao, S. C., & Sur, M. (1996). Orientation maps of subjective contours in visual cortex. *Science*, 274, 2110–2115.
- Simoncelli, E. P., & Olshausen, B. A. (2001). Natural image statistics and neural representation. *Annual Review Neuroscience*, 24, 1193–1216.
- Smith, A. T., Greenlee, M. W., Singh, K. D., Kraemer, F. M., & Hennig, J. (1998). The processing of first- and second-order motion in human visual cortex assessed by functional magnetic resonance imaging (fMRI). *Journal of Neuroscience*, 18, 3816–3830.
- Smith, A. T., & Scott-Samuel, N. E. (2001). First-order and second-order signals combine to improve perceptual accuracy. *Journal of the Optical Society of America A*, 18, 2267–2272.
- Song, Y., & Baker, C. L. Jr., (2005). Neural mechanisms mediating responses to abutting gratings: Luminance edges vs. illusory contours. *Visual Neuroscience*, 23, 181–199.
- Vaina, L. M., Makris, N., Kennedy, D., & Cowey, A. (1998). The selective impairment of the perception of first-order motion by unilateral cortical brain damage. *Visual Neuroscience*, 15, 333–348.
- von der Heydt, R., & Peterhans, E. (1989). Mechanisms of contour perception in monkey visual cortex. I. Lines of pattern discontinuity. *Journal of Neuroscience*, 9, 1731–1748.
- Whitaker, D., McGraw, P. V., Keeble, D. R. T., & Skillen, J. (2004). Pulling the other one: First- and second-order information interact to determine perceived position. *Vision Research*, 44, 279–286.
- Zhan, C. A., & Baker, C. L. Jr., (2006). Boundary cue invariance in cortical orientation maps. *Cerebral Cortex*, 16, 896–906.
- Zhou, Y.-X., & Baker, C. L. Jr., (1996). Spatial properties of envelope responses in Area 17 and 18 of the Cat. *Journal of Neurophysiology*, 75, 1038–1050.